Interannual variability and trends in tropical ozone derived from SAGE II satellite data and SHADOZ ozonesondes

William J. Randel[1] and Anne M. Thompson[2]

Received 13 October 2010; revised 13 January 2011; accepted 31 January 2011; published 6 April 2011.

[1] Long-term observations of stratospheric ozone from the Stratospheric Aerosol and Gas Experiment II (SAGE II) satellite (1984–2005) are combined with ozonesonde measurements from the Southern Hemisphere Additional Ozonesondes (SHADOZ) network (1998–2009) to study interannual variability and trends in tropical ozone. Excellent agreement is found comparing the two data sets for the overlap period 1998–2005, and the data are combined to form a continuous time series covering 1984–2009. SHADOZ measurements also provide temperature profiles, and interannual changes in ozone and temperature are highly correlated throughout the tropical lower stratosphere (16–27 km). Interannual variability in stratospheric ozone is dominated by effects of the quasi-biennial oscillation and El Niño–Southern Oscillation, and there are also significant negative trends (−2 to −4% per decade) in the tropical lower stratosphere (over 17–21 km). These tropical ozone trends are consistent with results from chemistry-climate model simulations, wherein the trends result from increases in upwelling circulation in the tropical lower stratosphere.

Citation: Randel, W. J., and A. M. Thompson (2011), Interannual variability and trends in tropical ozone derived from SAGE II satellite data and SHADOZ ozonesondes, *J. Geophys. Res.*, *116*, D07303, doi:10.1029/2010JD015195.

1. Introduction

[2] Quantifying ozone variability and trends from historical observations is a key component to understanding past changes and validating models used to predict future evolution of global ozone. While the tropics cover a large fraction of the globe, there are few data sets that provide long-term observations of ozone with high vertical resolution over the tropics. One particularly useful long-term record for stratospheric ozone was provided by the Stratospheric Aerosol and Gas Experiment II (SAGE II) satellite instrument, which operated from 1984 to 2005. These high-quality observations, based on solar occultation measurements, provided the basis for monitoring global ozone variability and trends over two decades, and formed a benchmark for UNEP/WMO Ozone Assessments [e.g., *World Meteorological Organization (WMO)*, 2006]. The SAGE II data have also been combined with measurements from the previous SAGE I instrument (1979–1982) to extend the record, although there are uncertainties in combining data from nonoverlapping (in time) satellite instruments. Unfortunately the SAGE II data record ended in 2005, and subsequent satellite instruments have very different vertical resolution and sampling patterns which hamper construction of a continuous global satellite record.

[1]National Center for Atmospheric Research, Boulder, Colorado, USA.
[2]Department of Meteorology, Pennsylvania State University, University Park, Pennsylvania, USA.

0148-0227/11/2010JD015195

[3] Beginning in 1998 a series of ozonesonde stations was established in the tropics to provide regular ozone observations in this historically poorly sampled region. These stations are collectively termed the Southern Hemisphere Additional Ozonesonde (SHADOZ) network [*Thompson et al.*, 2003a], and consist of ~12 stations covering a range of longitudes over the latitude band ~10°N–20°S. This network of stations continues to provide regular measurements, with the time series for many locations now covering 1998–2010. There is a significant temporal overlap between the SHADOZ ozonesondes and SAGE II satellite observations (1998–2005). The objective of this paper is to explore combining these data sets to (1) document data quality for each data set (on the basis of the overlap period) and (2) construct a continuous data set for 1984–2009 to quantify interannual variability and trends for this extended record. As the SHADOZ measurements are expected to continue in the future, this combined data set will provide an opportunity to continue monitoring long-term ozone variability in the tropics.

[4] One key science topic addressed here regards long-term ozone trends in the tropical lower stratosphere. As noted above, there have been few long-term observational data sets to quantify such trends. Calculations using the combined SAGE I+II data reveal significant negative trends in this region [*Randel and Wu*, 2007], although there are uncertainties regarding the details of combining two separate (nonoverlapping) satellite data sets, and in addition the SAGE I data do not extend below 20 km. Furthermore, these trend results have not been validated using other ozone measurements. Decadal-scale ozone trends in the tropical lower stratosphere are especially interesting because they

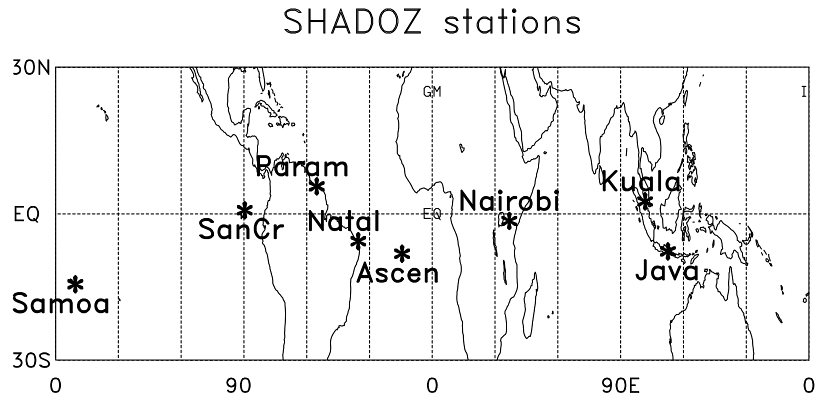

Figure 1. Location of the near-equatorial SHADOZ stations used in this study.

are found to occur in chemistry-climate model (CCM) simulations of the recent past [*Eyring et al.*, 2010, chapter 9], driven primarily by increases in tropical upwelling in the models (and not chemistry effects; see *Lamarque and Solomon* [2010]). Lower stratospheric ozone is especially sensitive to such upwelling changes because of the strong vertical gradient in this region. In fact, because there are no direct measurements of upwelling near the tropical tropopause, and there are large uncertainties in indirect measurements or assimilated data products [*Iwasaki et al.*, 2009], ozone observations can provide a sensitive measure of upwelling changes in the real atmosphere.

2. Data and Analysis

[5] The SAGE II satellite instrument provided high-quality vertical profiles of ozone on the basis of solar occultation measurements [*McCormick et al.*, 1989], with observations covering the period November 1984 to August 2005. The profiles span an altitude range from 15 to 50 km, with a vertical resolution of 1 km. The SAGE II data used here are based on the v6.2 retrieval algorithm, and the data are screened for cloud and aerosol contamination according to the procedure described in the work of *Wang et al.* [2002]. Data are omitted for 2 years following the volcanic eruption of Mt. Pinatubo in June 1991, when high levels of stratospheric aerosols influenced the SAGE retrievals [*Wang et al.*, 2002]. The SAGE II solar occultation measurements have relatively sparse spatial sampling, with 14 measurements per day over a narrow latitude range (which slowly progresses over one month to cover the latitude range ~55°N–S; see *McCormick et al.* [1989]). We analyze the SAGE II data binned into monthly samples, combining all measurements over 20°N–S. There was a slow drift in the SAGE II orbit, so that the tropical sampling changed slightly over time; there are some months with no observations prior to 1995, and less afterward.

[6] The SHADOZ ozone and pressure-temperature-wind profiles are collected by coupled ozonesonde-radiosonde instrumentation [*Thompson et al.*, 2003a, 2003b, 2007]. Owing to response times of the ozonesonde electrochemical concentration cell solution, the effective vertical resolution of the ozone data is 50–100 m, considerably better than SAGE II and other profiling satellites. The data used here are sampled with a 0.5 km vertical spacing. We focus on analysis of observations from 7 SHADOZ stations within +/−10° of the equator with long and continuous records; the seven sites are illustrated in Figure 1, along with Samoa (14°S; included in the ENSO analysis below). There are ~2–4 observations per month at each of the SHADOZ stations, which we combine in simple monthly averages for each station. The upper level of the ozonesonde observations can reach ~35 km, but the overall number of observations decreases rapidly with altitude above ~30 km, so that the sampling is limited for altitudes 30–35 km. The stratospheric segment of the ozone profile exhibits a high degree of longitudinal symmetry [*Thompson et al.*, 2003a],

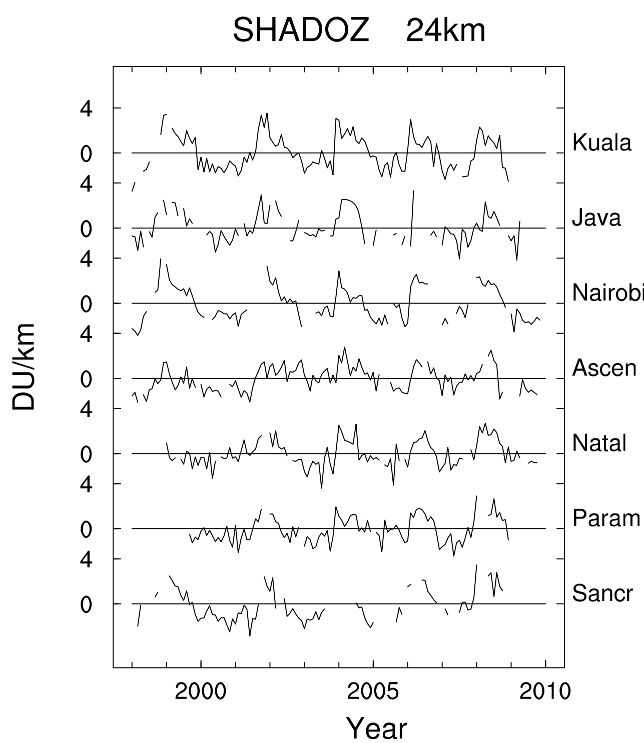

Figure 2. Time series of deseasonalized ozone anomalies at 24 km for each of 7 near-equatorial SHADOZ stations. Ozone density given in Dobson units (DU) per kilometer.

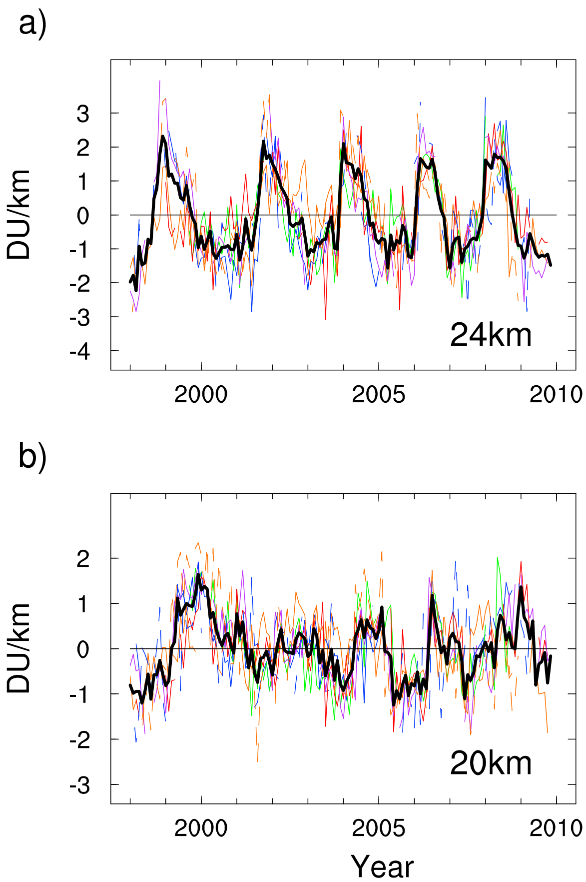

Figure 3. Time series of deseasonalized ozone anomalies from SHADOZ data at (a) 24 km and (b) 20 km. Color lines show results from each of the seven SHADOZ stations in Figure 1, and the thick black line shows the average of the seven stations.

which facilitates averaging of the different SHADOZ stations for comparison and combining with the zonal mean SAGE II data. Both the SAGE II and SHADOZ data are deseasonalized by removing the respective long-term monthly means, and in all of the analysis below we focus on deseasonalized anomalies.

3. Results

3.1. SHADOZ Data

[7] Time series of deseasonalized ozone anomalies at 24 km for each of the7 SHADOZ stations is shown in Figure 2. The predominant variability in Figure 2 is an approximate 2 year cycle linked to the quasi-biennial oscillation (QBO), and the time series show similar sized variations and an approximate in-phase behavior among the different stations. This behavior is further illustrated in Figure 3a, where the 24 km anomalies from the individual stations are overlaid, together with the 7 station average. A corresponding result for 20 km is shown in Figure 3b, which also shows correlated interannual variability among the different stations. Hereafter we focus on the seven station average anomalies (black lines in Figure 3) to represent the SHADOZ tropical ozone anomalies.

[8] Figure 4a shows a height-time section of the SHADOZ ozone anomalies (in terms of ozone density, in Dobson units (DU)/km) for the entire 1998–2009 record. This shows the clear signature of downward propagating anomalies linked to the QBO, with large amplitudes over ~20–27 km. Smaller amplitude variations are observed in the middle stratosphere (~28–35 km), approximately out of phase with the lower stratosphere. This behavior is consistent with

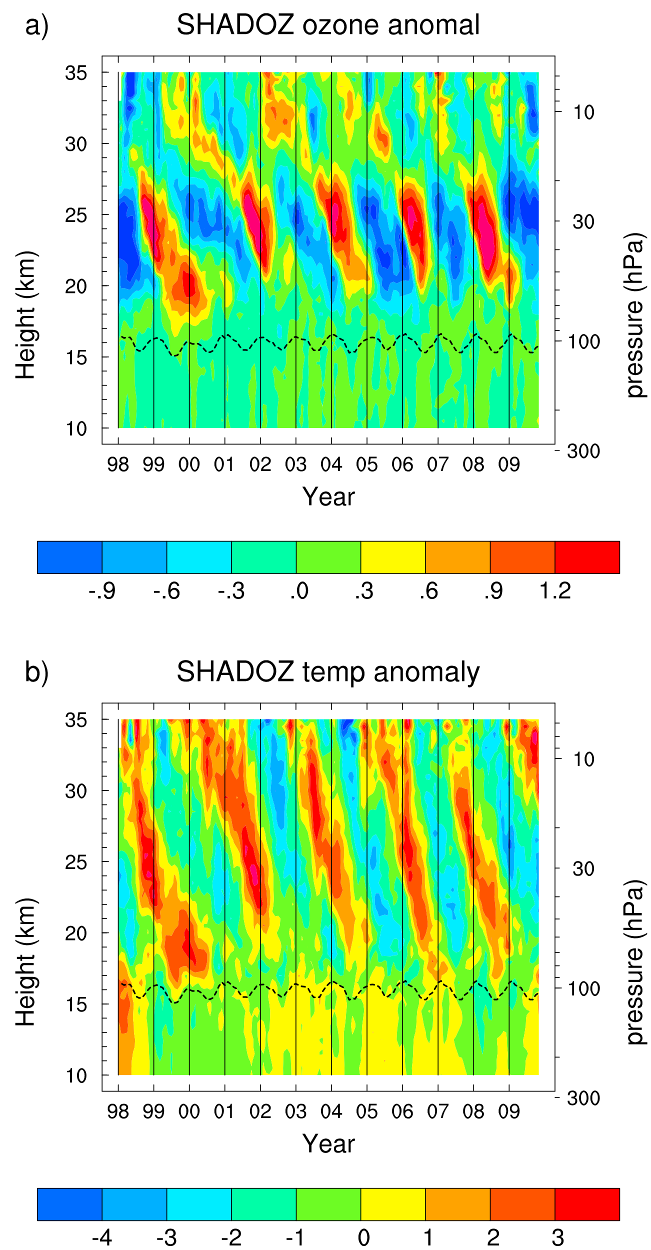

Figure 4. Height-time sections of deseasonalized anomalies in (a) ozone (Dobson units (DU) per kilometer) and (b) temperature (K) from SHADOZ measurements during 1998–2009. Results are derived from an average of seven stations, as in Figure 2. The thin dashed black line denotes the tropical tropopause.

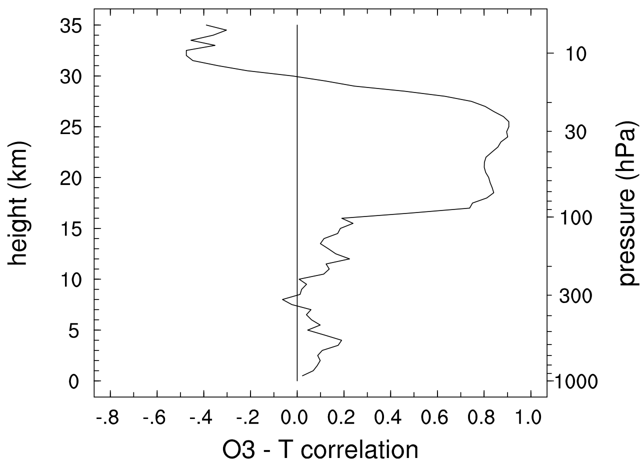

Figure 5. Vertical profile of correlation between combined (seven-station average) SHADOZ ozone and temperature anomalies over 1998–2009 (data from Figure 3). The approximate 95% significance level is near 0.17.

previous analyses of the ozone QBO [*Chipperfield et al.*, 1994; *Randel and Wu*, 1996; *Logan et al.*, 2003; *Witte et al.*, 2008; *Lee et al.*, 2010], and is linked to dynamical versus chemical control of ozone in the lower and middle-upper stratosphere, respectively. There are also some irregular ozone variations in the lower stratosphere in Figure 4a (i.e., the large positive anomaly in 1999–2000), which are linked to the combined effects of the QBO and ENSO (as shown below).

[9] An equivalent height-time section of temperature anomalies is shown in Figure 4b, constructed from an average of the individual SHADOZ temperature measurements (analogous to Figure 3a). The temperature data show coherent QBO variations of +/−3K with continuous downward propagation throughout the middle and lower stratosphere (~35–20 km). The temperature patterns are highly correlated with ozone over altitudes ~16–27 km (Figure 5), and anticorrelated over 30–35 km. Note that the irregular ozone variations in the lowermost stratosphere (~17–21 km) are echoed in correlated temperature anomalies in Figure 4.

3.2. Combined SHADOZ and SAGE II Data

[10] Time series of the SAGE II and SHADOZ ozone anomalies at 20, 24 and 32 km are shown in Figure 6, including the overlap period covered by both measurements (1998–2005). The time series in Figure 6 have been constructed by setting the time average for the overlap period equal to zero for each data set. The comparisons for the overlap period show remarkably good agreement between the SAGE II and SHADOZ anomalies, with correlations of order 0.8–0.9 over altitudes ~18–27 km (where the largest variability occurs), and 0.4–0.6 for altitudes 28–35 km (where, as noted above, the ozonesonde sampling becomes limited). This agreement prompts confidence in the quality of each data set independently, and also suggests it is reasonable to combine the data to form a continuous time series over 1984–2009. We create a single time series from the combined data by simply averaging the SAGE II and SHADOZ results for the overlap period.

[11] Time series of the combined data are shown in Figure 7, highlighting ozone variations over altitudes 17–21, 22–28 and 29–35 km. Largest QBO variations (of +/−10 DU) occur over 22–28 km, and this accounts for the majority of the QBO signal observed in equatorial column ozone [*Randel and Wu*, 1996]. Although less evident to the eye, smaller amplitude QBO variations are also embedded in the time series for 17–21 and 29–35 km, as shown in the regression analysis below.

[12] Components of variability in the combined SAGE II and SHADOZ data are analyzed using a standard multivariate linear regression analysis, including terms representing long-

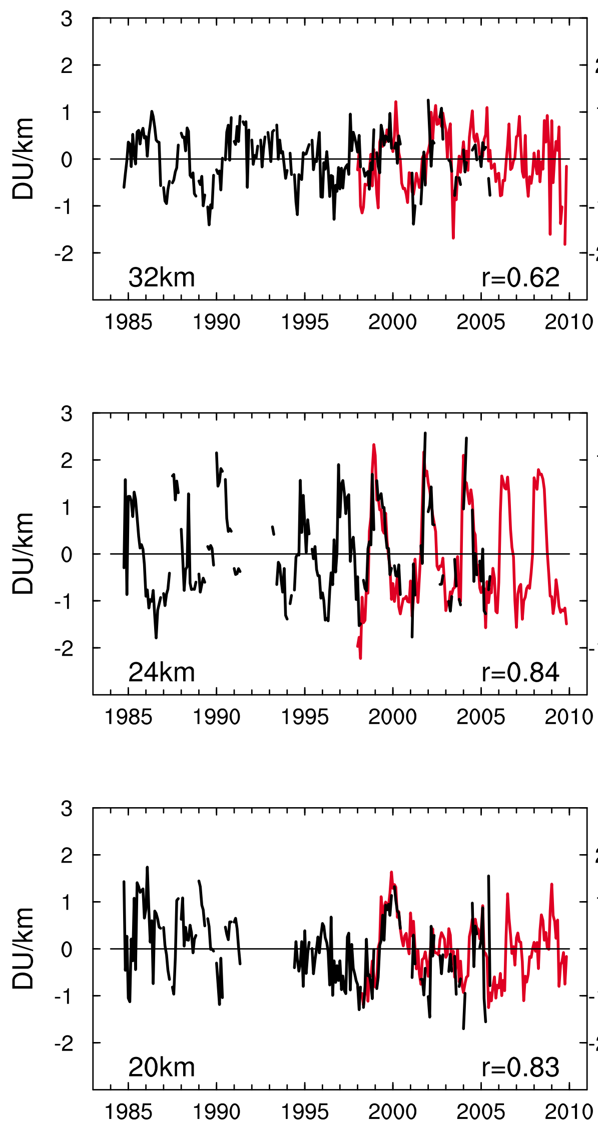

Figure 6. Time series of deseasonalized ozone anomalies at 20, 24, and 32 km, combining results from SAGE II (black lines) and SHADOZ data (red lines). The left axes denote ozone concentration in DU per kilometer, and the right axes indicate the relative percentage variations at each altitude. The time series of these data overlap for the period 1998–2005, and the correlation between the two data sets is noted in each panel.

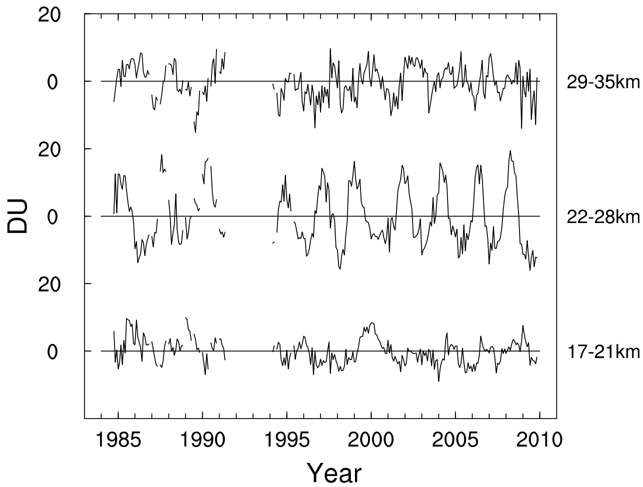

Figure 7. Time series of ozone anomalies (DU) from combined SAGE II and SHADOZ data for altitude layers 17–21, 22–28, and 29–35 km.

term linear trend, 11 year solar cycle, QBO and ENSO variability [e.g., *Randel and Wu*, 2007]. We use a linear trend basis function for the long-term changes, rather than a term proportional to equivalent effective stratospheric chlorine (EESC), for simplicity of analysis and interpretation, plus acknowledgment of the fact that EESC is less well defined for the tropical lower stratosphere [*Lary et al.*, 2007]. The solar cycle proxy (10.7 cm radio index) is included as a standard regression term for stratospheric ozone, although we find little evidence of statistically significant results for these tropical data, and the solar term is not discussed further here. QBO variability is based on two orthogonal QBO time series [*Wallace et al.*, 1993; *Randel and Wu*, 1996], and ENSO variability is based on the Multivariate ENSO Index (MEI) obtained from the NOAA Climate Diagnostics Center (see http://www.cdc.noaa.gov/people/klaus.wolter/MEI/) with atmospheric variables lagged by two months. Uncertainty estimates for the statistical fits are calculated using a bootstrap resampling technique [*Efron and Tibshirani*, 1993], which includes the effects of serial autocorrelation. Note that the period following the

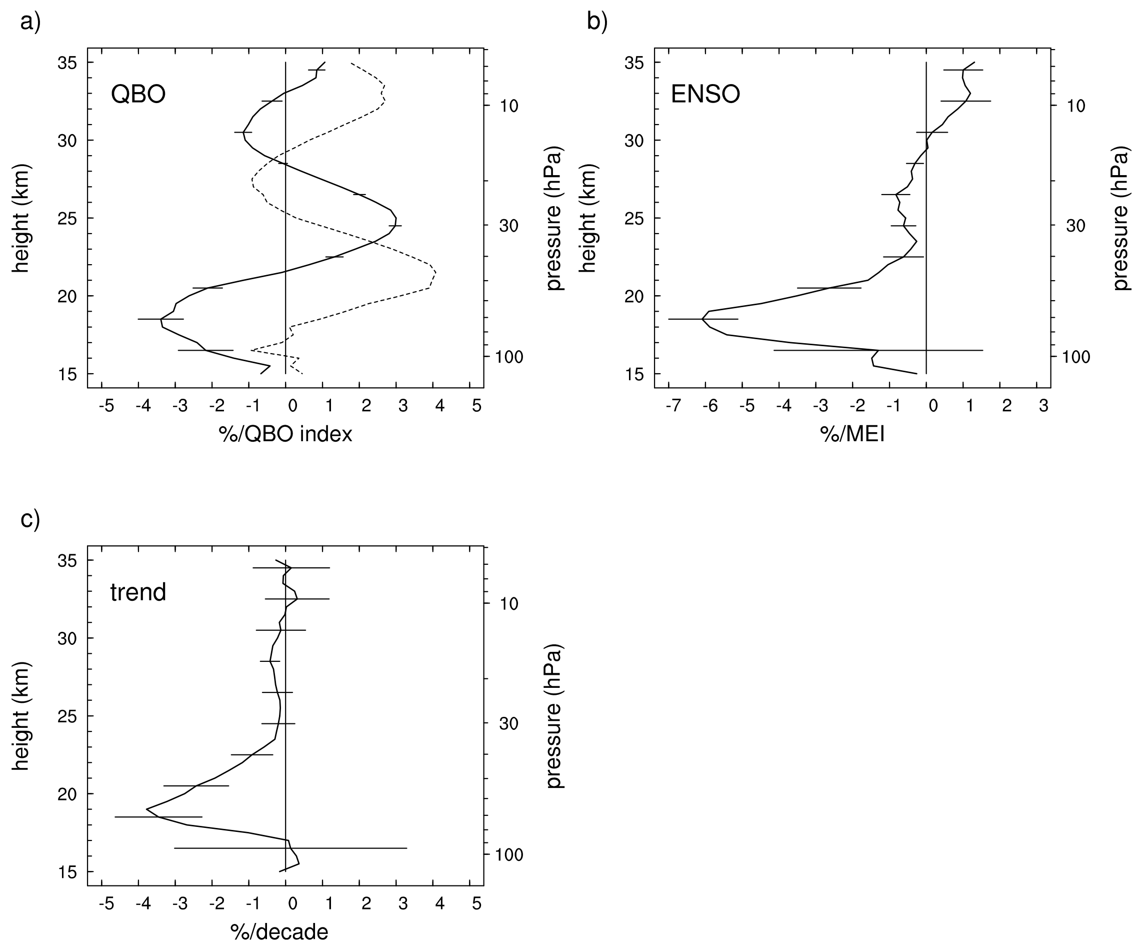

Figure 8. Vertical profile of components of ozone variability in combined SAGE II and SHADOZ data derived from regression analysis. Results are shown for (a) the two orthogonal components of the quasi-biennial oscillation (QBO; units of percent ozone per unit of normalized QBO index), (b) ENSO (percent ozone per normalized Multivariate ENSO Index (MEI)), and (c) linear trends (percent ozone per decade). Error bars denote two-sigma statistical uncertainties in the regression fits.

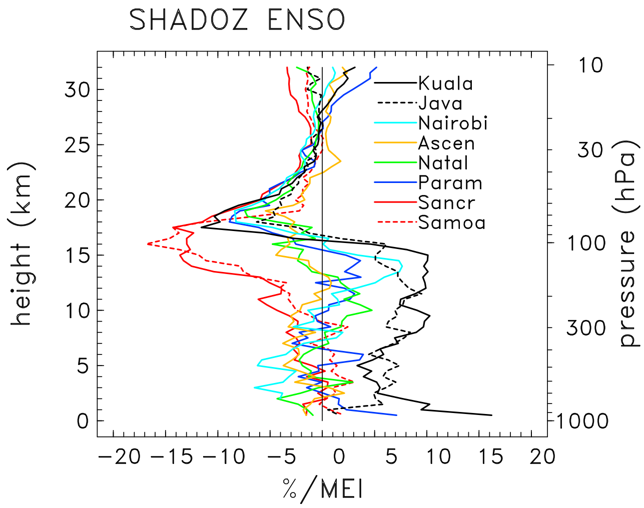

Figure 9. Vertical profiles of ENSO projection of ozone variability for each of eight SHADOZ stations (during 1998–2009) covering altitudes 0–30 km. Units are percent ozone per normalized Multivariate ENSO Index (MEI).

eruption of Mt. Pinatubo is effectively excluded in this analysis because of the missing SAGE II observations. As a note, the regression model accounts for ~60–80% of the overall variance in the combined SAGE II and SHADOZ data for altitudes 20–27 km, and smaller fractions (20–40%) above and below.

[13] Figure 8 shows vertical profiles of the regression fits for the QBO, ENSO and trend variations, with results expressed as local percent variations (compared to the background time average vertical profile). The QBO shows statistically significant components over the entire depth of the stratosphere (16–35 km); the global behavior of the ozone QBO is discussed in further detail in the work of *Randel and Wu* [2007]. The ENSO pattern exhibits a large negative signal in the lower stratosphere (~17–21 km), with magnitude approximately −6% per standard MEI index. This is similar to the result for the SAGE II data alone, and this is also consistent with ENSO variations found in chemistry climate model simulations [*Randel et al.*, 2009]. This variability is interpreted as a coherent decrease in tropical ozone associated with enhanced tropical upwelling during so-called ENSO warm events [*Randel et al.*, 2009; *Calvo et al.*, 2010].

[14] The combined SAGE II and SHADOZ data cover the altitude range 15–35 km, but the ENSO variability can be explored over a broader altitude range 0–35 km on the basis of the shorter record of SHADOZ data alone (1998–2009). Figure 9 shows the results of a similar regression fit for ENSO for this period, including results for each of the individual SHADOZ stations (and additionally including Samoa). As a note, there is some substantial correlation between the MEI and QBO proxies for this short 1998–2009 record (up to +/−0.35), so that there could be possible confusion of these signals in the stratosphere, although this is probably not a large effect. Each of the stations shows a negative ENSO projection in the lower stratosphere, similar to the result in Figure 8b, demonstrating that this is mainly a longitude-independent (zonal mean) signal. In contrast, there is a wide range of ENSO projections in the upper troposphere (~10–16 km), with strong negative signals in the eastern Pacific (Samoa and San Cristobal), positive signals over Indonesia (Kuala Lumpur and Java), and smaller signals elsewhere. This longitudinally dependent response of tropical tropospheric ozone to ENSO variability is consistent with structure derived from previous analysis of satellite observations [*Chandra et al.*, 1998; *Ziemke and Chandra*, 2003; *Logan et al.*, 2008; *Ziemke et al.*, 2010]. In particular, these studies document a response to ENSO warm events of increased tropospheric ozone over Indonesia and the western Pacific ocean, coupled with a decrease in ozone over the eastern Pacific. These variations are linked to ENSO-associated changes in burning and surface emissions, deep convective transport, plus photochemical response to variations in upper tropospheric water vapor [*Chandra et al.*, 1998; *Fujiwara et al.*, 1999; *Thompson et al.*, 2001; *Sudo and Takahashi*, 2001]. We note that the results in Figure 9 (based on a relatively short observational record) suggest somewhat different vertical structure response for the Indonesian ozone increases (over ~7–15 km) versus eastern Pacific decreases (mainly in the TTL, ~13–17 km; see also *Lee et al.* [2010]).

[15] Figure 10 shows a similar calculation of the ENSO signal in temperature for each of the SHADOZ stations. Here the behavior is similar to that for ozone in the lower stratosphere, with a coherent negative ENSO signal evident at each station (peaking near 18–19 km); that is, cold stratospheric anomalies during so-called ENSO warm events. However, in contrast to the ozone behavior in Figure 9, the ENSO temperature signal in the upper troposphere is more similar among the different stations, with positive projections (i.e., warm anomalies for ENSO warm events) which increase with altitude from lower levels. This tropospheric temperature response is consistent with well-known behavior for ENSO [e.g., *Reid et al.*, 1989; *Yulaeva and*

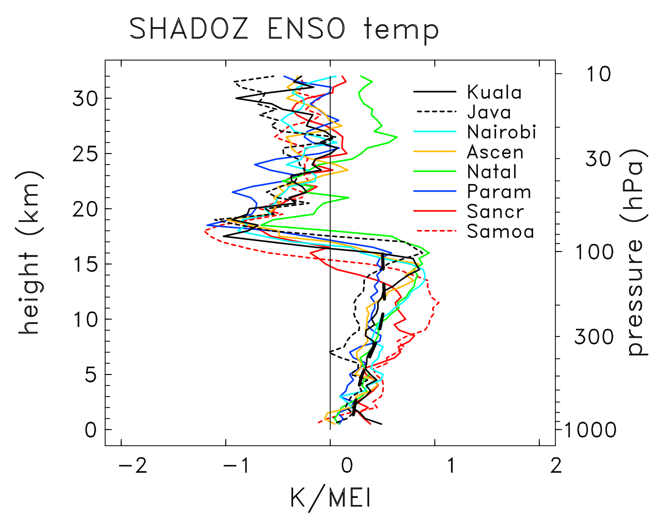

Figure 10. Vertical profiles of ENSO projection of temperature variability for the individual SHADOZ stations, as in Figure 9. Units are K per normalized Multivariate ENSO Index (MEI). Heavy dashed line indicates the vertical structure of an approximate moist adiabat.

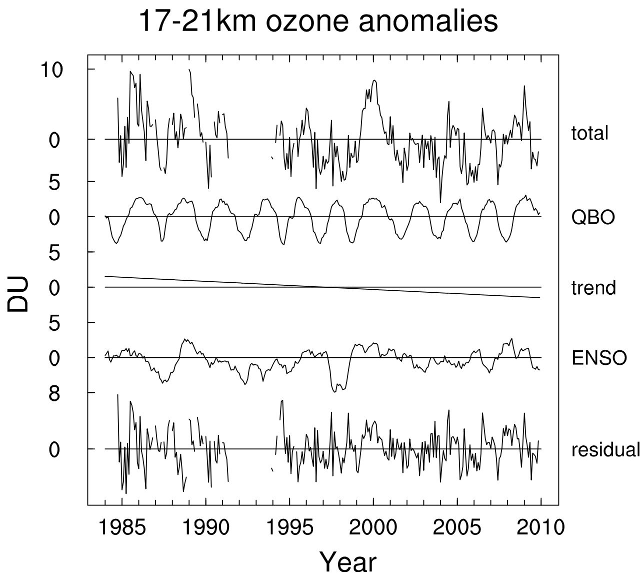

Figure 11. Top curve shows time series of SAGE II and SHADOZ ozone anomalies (in DU) for the 17–21 km layer. Lower curves show components of variability associated with QBO, trend and ENSO components, derived from linear regression, together with the residual.

Wallace, 1994]; note that the vertical structure of the tropospheric temperature is reasonably consistent with a moist adiabatic temperature response [e.g., *Santer et al.*, 2005].

[16] The long-term trend projection of the SAGE II and SHADOZ data (Figure 8c) shows a statistically significant negative trend in the lower stratosphere, peaking near 17–21 km, with a maximum near −4% per decade at 19 km. This is similar to the negative trends in the tropical lower stratosphere evident in the combined SAGE I+II data in the work of *Randel and Wu* [2007]. Overall the regression results show that the QBO, ENSO and trend components all contribute significant variability for lower stratosphere ozone. This is illustrated in the time series of ozone for the 17–21 km layer in Figure 11, showing each of the QBO, ENSO and trend components, together with the residual to the regression fit. Large anomalies in the observed time series often correspond to in-phase variations of the QBO and ENSO signals (e.g., 1988–1989 and 1999–2000). Overall nearly identical behavior is observed for lower stratospheric temperatures [*Randel et al.*, 2009, Figure 4], consistent with the strong coherence between ozone and temperature in this region shown in Figures 4–5. While the QBO, ENSO and trend components are all statistically significant for the time series in Figure 11 (see Figure 8), the residual ozone variability is relatively large. We note that the nature of this residual variability (i.e., some combination of natural high-frequency fluctuations versus observational uncertainties) is not well understood at present.

4. Summary and Discussion

[17] The SAGE II satellite instrument had a remarkable lifetime of over two decades, but ceased operation in 2005, and since this time there are not similar high vertical resolution (~1 km) satellite measurements of tropical ozone available. This study has explored the utility of combining the SAGE II observations with tropical measurements from the SHADOZ ozonesonde network, to study interannual variability and trends. There is a long overlap period between the two data sets (1998–2005), and comparisons show excellent agreement (Figure 6). This agreement fosters confidence in each of the separate data sets, and prompts combining the data to create a single time series over 1984–2009.

[18] Variability in tropical stratospheric ozone is primarily linked to the QBO and ENSO, consistent with previous results [e.g., *Shiotani and Hasebe*, 1994]. The SHADOZ data record now covers over 5 complete QBO cycles, and the complementary temperature measurements reveal high correlation between ozone and temperature over altitudes 16–27 km. ENSO variability in ozone is mainly evident as a zonal mean response in the tropical lower stratosphere (~17–21 km), with typical variations of ~10% local background levels (and strong correlation to temperature). The interpretation is that these ozone and temperature changes are linked to enhanced zonal mean tropical stratospheric upwelling in ENSO warm events [*Randel et al.*, 2009; *Calvo et al.*, 2010]. The ozone ENSO signal derived from the SAGE II and SHADOZ record is reasonably consistent with results from recent chemistry-climate model (CCM) simulations forced by imposed sea surface temperatures, as shown in the work of *Randel et al.* [2009]. Overall similar behavior is found for other CCM simulations [*Eyring et al.*, 2010, chapter 8].

[19] The SHADOZ data also allow examination of the ENSO influence on tropical tropospheric ozone, albeit for a shorter record (1998–2009). Results show a strongly longitudinally dependent behavior, with out-of-phase patterns between the Indonesian/western Pacific and eastern Pacific regions. This behavior is consistent with previous satellite-based results, which were mainly focused on tropospheric column ozone [*Chandra et al.*, 1998; *Ziemke and Chandra*, 2003; *Logan et al.*, 2008; *Ziemke et al.*, 2010]. The relatively short record of SHADOZ data suggests distinct vertical structure for these different regions (Figure 9), and a continuing record from SHADOZ may allow more detailed understanding of tropospheric ozone vertical structure linked to ENSO.

[20] The combined SAGE II and SHADOZ data also exhibit statistically significant negative trends in the tropical lower stratosphere (approximately −2 to −4% per decade over ~17–21 km). As noted in the Introduction, such an ozone trend is simulated in many current chemistry-climate models, as a result of systematic increased tropical stratospheric upwelling [*Eyring et al.*, 2010, chapter 9; *Lamarque and Solomon*, 2010]. Figure 12 shows a comparison of the SAGE II and SHADOZ trends with trend results from twelve different CCMval2 simulations from *Eyring et al.* [2010], derived for the period 1980–2005 using a multivariate regression analysis. As a note, results from six other CCMval2 models were not included in Figure 12, because the trends were substantially different (outliers) from the group shown. The results in Figure 12 show a reasonably similar vertical structure and magnitude of trends between the SAGE II and SHADOZ results and the models. The SAGE II and SHADOZ trends are somewhat more negative and centered slightly higher in altitude than the model results,

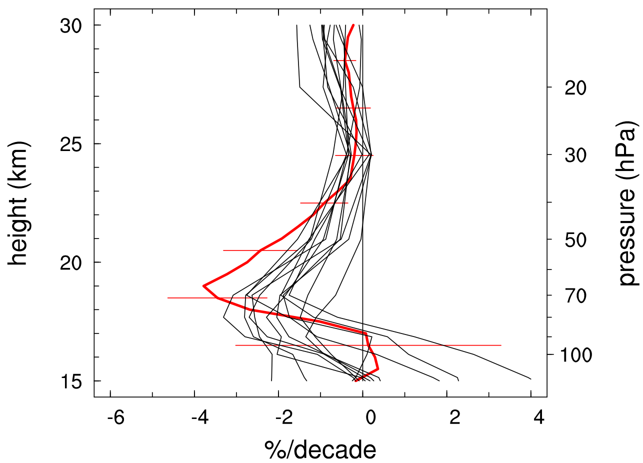

Figure 12. Vertical profile of ozone trends (in percent per decade) derived from SAGE II and SHADOZ data (red line, from Figure 8c), together with ozone trends derived from twelve CCMval2 chemistry-climate model simulations for the period 1980–2005.

but note that most of these models do not include detailed tropospheric ozone chemistry, and hence are not expected to simulate realistic behavior for altitudes near and below the tropopause (~17 km). One interpretation of the agreement in Figure 12 is that there have been increases in tropical upwelling in the real atmosphere for the most recent 25 years, comparable in magnitude (and somewhat larger) to those simulated in the CCMval2 model results (the upwelling increases in the models are of the order 2% per decade; see *Eyring et al.* [2010, chapter 4].

[21] This study has demonstrated the utility of regular measurements from the SHADOZ network for monitoring interannual variability and trends in tropical ozone, and these are likely to be the primary source of high vertical resolution tropical ozone measurements for the foreseeable future. As such, it will be important to maintain the SHADOZ measurements on a regular and continuing basis.

[22] **Acknowledgments.** We thank Masatomo Fujiwara, J. F. Lamarque, and Simone Tilmes for constructive reviews and comments on the manuscript. Most of the data processing was performed by Fei Wu at NCAR. This work was partially supported by the NASA ACMAP Program (W.J.R.) and the NASA Aura Validation and Upper Atmosphere Research Projects (A.M.T.). NCAR is operated by the University Corporation for Atmospheric Research under sponsorship of the National Science Foundation.

References

Calvo, N., R. R. Garcia, W. J. Randel, and D. Marsh (2010), Dynamical mechanism for the increase in tropical upwelling in the lowermost tropical stratosphere during warm ENSO events, *J. Atmos. Sci.*, *67*, 2331–2340, doi:10.1175/2010JAS3433.1.

Chandra, S., J. R. Ziemke, W. Min, and W. G. Read (1998), Effects of 1997–1998 El Niño on tropospheric ozone and water vapor, *Geophys. Res. Lett.*, *25*, 3867–3870, doi:10.1029/98GL02695.

Chipperfield, M. P., L. J. Gray, J. S. Kinnersley, and J. Zawodny (1994), A two-dimensional model study of the QBO signal in SAGE II NO_2 and O_3, *Geophys. Res. Lett.*, *21*, 589–592, doi:10.1029/94GL00211.

Efron, B., and R. J. Tibshirani (1993), *An Introduction to the Bootstrap*, 436 pp., Chapman and Hall, New York.

Eyring, V., T. G. Shepherd, and D. W. Waugh (Eds.) (2010), Report on the evaluation of chemistry-climate models, *SPARC Rep. 5, WCRP-132, WMO/TD 1526*, Stratospheric Processes and Their Role in Clim., World Clim. Res. Programme, Geneva. (Available at http://www.atmosp.physics.utoronto.ca/SPARC.)

Fujiwara, M., K. Kita, S. Kawakami, T. Ogawa, N. Komala, S. Saraspriya, and A. Suripto (1999), Tropospheric ozone enhancements during the Indonesian forest fire events in 1994 and in 1997 as revealed by ground-based observations, *Geophys. Res. Lett.*, *26*, 2417–2420, doi:10.1029/1999GL900117.

Iwasaki, T., H. Hamada, and K. Miyazaki (2009), Comparisons of Brewer-Dobson circulations diagnosed from reanalyses, *J. Meteorol. Soc. Jpn.*, *87*, 997–1006, doi:10.2151/jmsj.87.997.

Lamarque, J. F., and S. Solomon (2010), Impact of changes in climate and halocarbons on recent lower stratospheric ozone and temperature trends, *J. Clim.*, *23*, 2599–2611, doi:10.1175/2010JCLI3179.1.

Lary, D. J., D. W. Waugh, A. R. Douglass, R. S. Stolarski, P. A. Newman, and H. Mussa (2007), Variations in stratospheric inorganic chlorine between 1991 and 2006, *Geophys. Res. Lett.*, *34*, L21811, doi:10.1029/2007GL030053.

Lee, S., D. M. Shelow, A. M. Thompson, and S. K. Miller (2010), QBO and ENSO variability in temperature and ozone from SHADOZ, 1998–2005, *J. Geophys. Res.*, *115*, D18105, doi:10.1029/2009JD013320.

Logan, J. A., D. B. A. Jones, I. A. Megretskaia, S. J. Oltmans, B. J. Johnson, H. Vömel, W. J. Randel, W. Kimani, and F. J. Schmidlin (2003), Quasi-biennial oscillation in tropical ozone as revealed by ozonesonde and satellite data, *J. Geophys. Res.*, *108*(D8), 4244, doi:10.1029/2002JD002170.

Logan, J. A., I. Megretskaia, R. Nassar, L. T. Murray, L. Zhang, K. W. Bowman, H. M. Worden, and M. Luo (2008), Effects of the 2006 El Niño on tropospheric composition as revealed by data from the Tropospheric Emission Spectrometer (TES), *Geophys. Res. Lett.*, *35*, L03816, doi:10.1029/2007GL031698.

McCormick, M. P., J. M. Zawodny, R. E. Viega, J. C. Larson, and P. H. Wang (1989), An overview of SAGE I and II ozone measurements, *Planet. Space Sci.*, *37*, 1567–1586, doi:10.1016/0032-0633(89)90146-3.

Randel, W. J., and F. Wu (1996), Isolation of the ozone QBO in SAGE II data by singular value decomposition, *J. Atmos. Sci.*, *53*, 2546–2559, doi:10.1175/1520-0469(1996)053<2546:IOTOQI>2.0.CO;2.

Randel, W. J., and F. Wu (2007), A stratospheric ozone profile data set for 1979–2005: Variability, trends, and comparisons with column ozone data, *J. Geophys. Res.*, *112*, D06313, doi:10.1029/2006JD007339.

Randel, W. J., R. R. Garcia, N. Calvo, and D. Marsh (2009), ENSO influence on zonal mean temperature and ozone in the tropical lower stratosphere, *Geophys. Res. Lett.*, *36*, L15822, doi:10.1029/2009GL039343.

Reid, G., K. Gage, and J. McAfee (1989), The thermal response of the tropical atmosphere to variations in equatorial Pacific sea surface temperature, *J. Geophys. Res.*, *94*, 14,705–14,716.

Santer, B. D., et al. (2005), Amplification of surface temperature trends and variability in the tropical atmosphere, *Science*, *309*, 1551–1556, doi:10.1126/science.1114867.

Shiotani, M., and F. Hasebe (1994), Stratospheric ozone variations in the equatorial region as seen in stratospheric aerosol and gas experiment data, *J. Geophys. Res.*, *99*, 14,575–14,584, doi:10.1029/94JD00741.

Sudo, K., and M. Takahashi (2001), Simulation of tropospheric ozone changes during 1997–1998 El Niño: Meteorological impact on tropospheric photochemistry, *Geophys. Res. Lett.*, *28*, 4091–4094, doi:10.1029/2001GL013335.

Thompson, A. M., J. C. Witte, R. D. Hudson, H. Guo, J. R. Herman, and M. Fujiwara (2001), Tropical tropospheric ozone and biomass burning, *Science*, *291*, 2128–2132, doi:10.1126/science.291.5511.2128.

Thompson, A. M., et al. (2003a), Southern Hemisphere Additional Ozonesondes (SHADOZ) 1998–2000 tropical ozone climatology: 1. Comparison with Total Ozone Mapping Spectrometer (TOMS) and ground-based measurements, *J. Geophys. Res.*, *108*(D2), 8238, doi:10.1029/2001JD000967.

Thompson, A. M., et al. (2003b), Southern Hemisphere Additional Ozonesondes (SHADOZ) 1998–2000 tropical ozone climatology: 2. Tropospheric variability and the zonal wave-one, *J. Geophys. Res.*, *108*(D2), 8241, doi:10.1029/2002JD002241.

Thompson, A. M., J. C. Witte, H. G. J. Smit, S. J. Oltmans, B. J. Johnson, V. W. J. H. Kirchhoff, and F. J. Schmidlin (2007), Southern Hemisphere Additional Ozonesondes (SHADOZ) 1998–2004 tropical ozone climatology: 3. Instrumentation, station-to-station variability, and evaluation with simulated flight profiles, *J. Geophys. Res.*, *112*, D03304, doi:10.1029/2005JD007042.

Wallace, J. M., R. L. Panetta, and J. Estberg (1993), Representation of the equatorial quasi-biennial oscillation in EOF phase space, *J. Atmos. Sci.*, *50*, 1751–1762, doi:10.1175/1520-0469(1993)050<1751:ROTESQ>2.0.CO;2.

Wang, H. J., D. M. Cunnold, L. W. Thomason, J. M. Zawodny, and G. E. Bodeker (2002), Assessment of SAGE version 6.1 ozone data quality, *J. Geophys. Res.*, *107*(D23), 4691, doi:10.1029/2002JD002418.

Witte, J. C., M. R. Schoeberl, A. R. Douglass, and A. M. Thompson (2008), The Quasi-biennial Oscillation in tropical ozone from SHADOZ and HALOE, *Atmos. Chem. Phys.*, *8*, 3929–3936, doi:10.5194/acp-8-3929-2008.

World Meteorological Organization (WMO) (2006), Scientific assessment of ozone depletion: 2006, *Rep. 47*, Global Ozone Res. Monit. Proj., Geneva.

Yulaeva, E., and J. M. Wallace (1994), The signature of ENSO in global temperature and precipitation fields derived from the microwave sounding unit, *J. Clim.*, *7*, 1719–1736, doi:10.1175/1520-0442(1994)007<1719:TSOEIG>2.0.CO;2.

Ziemke, J. R., and S. Chandra (2003), La Niña and El Niño–induced variabilities of ozone in the tropical lower atmosphere during 1970–2001, *Geophys. Res. Lett.*, *30*(3), 1142, doi:10.1029/2002GL016387.

Ziemke, J. R., S. Chandra, L. D. Oman, and P. K. Bhartia (2010), A new ENSO index derived from satellite measurements of column ozone, *Atmos. Chem. Phys.*, *10*, 3711–3721, doi:10.5194/acp-10-3711-2010.

W. J. Randel, National Center for Atmospheric Research, 1850 Table Mesa Dr., PO Box 3000, Boulder, CO 80307, USA. (randel@ucar.edu)

A. M. Thompson, Department of Meteorology, Pennsylvania State University, 510 Walker Bldg., University Park, PA 16802, USA.